Zero-field paramagnetic resonance of trivalent gadolinium in several lanthanide tris(ethylsulfate) nonahydrates and nonadeuterates: Determination of crystal-field and hyperfine-structure parameters*†

E. R. Bernstein and G. M. Dobbs‡
Department of Chemistry, Princeton University, Princeton, New Jersey 08540
(Received 5 June 1974)

Employing isotopically pure trivalent ^{155}Gd, ^{157}Gd, and ^{160}Gd as impurities in dilute mixed crystals of lanthanum tris(ethylsulfate) nonahydrate [$La(C_2H_5SO_4)_3 \cdot 9H_2O$], it has been possible to determine both accurate zero-field splitting parameters of crystal-field origin and hyperfine-structure constants due to magnetic dipole and electric quadrupole interaction terms. The zero-field paramagnetic-resonance spectroscopic method employed herein, has allowed the absolute signs of the hyperfine parameters to be determined. Thus the magnitude and sign of all diagonal parameters of the zero-field effective spin Hamiltonian are accurately known. It is reasoned that the quadrupole hyperfine constant is due, almost entirely, to lattice contributions; moreover, it is shown to be of the expected order of magnitude and sign. The hyperfine anomaly is discussed and is shown to be slightly less than the experimental error limits (three standard deviations). A set of crystal-field parameters are reported for the first time for ^{160}Gd in crystals of $La(C_2H_5SO_4)_3 \cdot 9D_2O$, which differ significantly from those of the hydrate. Variations of crystal-field parameters with various lanthanide host ions are also observed. Finally, a few comments concerning zero-field linewidths and their measurement are made.

I. INTRODUCTION

Zero-field paramagnetic resonance (ZFPMR) is an important technique for observing magnetic-dipole transitions in the microwave region of the spectrum. These transitions are usually between energy levels split by crystal-field and hyperfine interactions in transition metal, lanthanide, and actinide ions. To date, such systems have been mainly studied by conventional electron-paramagnetic-resonance (EPR) spectroscopy in the presence of a strong Zeeman perturbation which forces differences in energy levels to match the energy of a source oscillator. In ZFPMR the microwave source is tuned to match the energy spacings of the sample. The data presented in this work emphasize the comparison between high- and zero-field paramagnetic resonance, particularly for improved hyperfine-structure resolution and crystal-field-splitting determinations.[1-13]

One of the long-standing problems of EPR spectroscopy of ions in crystals is that of the unexpected and unexplained crystal field and hyperfine structure of S-state ions (i.e., ions with half-filled shells such as $4f^7$), particularly in the lanthanide series. The usual lanthanide S-state ions are Eu^{2+}, Gd^{3+}, and Tb^{4+}; of these three $4f$ S-state ions Gd^{3+} is the most widely and readily obtainable chemically. Its lattice substitutional properties in a variety of trivalent-metal-ion crystal-host materials[14] makes Gd^{3+} an ideal choice for such a study. In the treatment of gadolinium paramagnetic resonance, a fictitious spin $\tilde{S}=\frac{7}{2}$ is used in conjunction with a spin Hamiltonian to describe the spectrum in an empirical manner. This convenient description is possible because the spectrum always displays the site symmetry of the ion. An exhaustive tabulation has been provided by Buckmaster and Shing.[15]

Many mechanisms have been proposed for the splitting, but no single one can account for the magnitude and sign of the observed splitting. This area of intense research has been many times reviewed and discussed in detail.[16,17] In order to evaluate a given theoretical mechanism for crystal-field splitting of the $^8S_{7/2}$ ground state of Gd^{3+}, the calculated over-all splitting should be compared with the measured value (this work)[18] 7258.4 ± 9.6 MHz for $La(C_2H_5SO_4)_3 \cdot 9H_2O : Gd^{3+}$.

All mechanisms proposed to account for crystal-field splitting of Gd^{3+} could, until very recently, be classified into three groups: much too large, much too small, and about the right magnitude but of the wrong sign.[16-20] However, using an effective operator technique, Newman and Urban[21] were able to calculate "intrinsic spin-Hamiltonian parameters." It is their contention that, due to geometric factors and a linear superposition of contributions from neighboring ligands, measured crystal-field parameters, especially quadrupolar ones, may or may not have the same sign as calculated (intrinsic) ones. It is clear that these concepts give both sign and rough order-of-magnitude agreement between crystal-field spin-Hamiltonian parameters obtained from theory and experiment.[21,22] The conclusion is that, at least for YVO_4, YPO_4, $LuPO_4$, $LuAsO_4$, and CaF_2, correlation and relativistic crystal-field effects contribute most significantly to the observed splittings. Indeed, these authors indicate that the previous calculation by Wybourne

when interpreted by their method, gives reasonable agreement between theory and experiment. Since the only quantitative treatment of these concepts has been for Gd^{+3}-H^- and Gd^{+3}-F^- in CaF_2 tetragonal sites, it still remains to be seen if general agreement for a larger number of situations will obtain.

It is possible that results presented herein can make a positive contribution to this area as the measured crystal-field parameters are different for $Ln(C_2H_5SO_4)_3 \cdot 9H_2O : Gd^{3+}$ and $Ln(C_2H_5SO_4)_3 \cdot 9D_2O : Gd^{3+}$ where Ln is a lanthanide.[23] Several mechanisms are suggested (end of Sec. III) by which this effect could occur.

Curiously enough, hyperfine structure was never conclusively observed for Gd^{3+} in these hosts in spite of its observation in many others. Since the spectral splittings produced are greater in zero than in high field when compared to the observed linewidths, it was possible to measure hyperfine constants for the first time. A detailed analysis of the spectrum and the constants themselves is presented in Secs. III and IV. The constants are discussed from the point of view of the theory of hyperfine interactions.

As a conclusion to this introduction, it is perhaps appropriate to mention at least briefly previous work on Gd^{3+} in the ethylsulfate-host-crystal system. The field has indeed had a long history commencing with studies in the late 1940's and early 1950's. The now famous work of Bleaney, Elliott, Stevens, and co-workers genuinely initiates EPR spectroscopy as a general physical technique for the study of solids.[24-28] Studies over the years have produced many interesting results for these salts.[29-34] The works that directly bear on the present investigation are an early work of Bleaney and co-workers[28] which suggested that the zero-field splitting (ZFS) *could not* be characterized by spin-Hamiltonian parameters obtained at high field; a ZFPMR[35] study of Gd^{3+} in lanthanum tris (ethylsulfate) nonahydrate (LES), of large experimental uncertainty (± 25 MHz in transition frequency), which indicated such a discrepency did not exist but which observed no hyperfine structure; a high-field experiment which demonstrated gadolinium-gadolinium and gadolinium-water proton coupling[36]; and finally, recent low-field measurements[37,38] reinvestigate the adequacy of fit of the high-field spin-Hamiltonian parameters to low-field spectra. One interesting aspect of these latter results is the suggestion that field-frequency plots for one of the transitions may be nonlinear in fields below 10 G.[38] Other work has been reviewed in Ref. 39.

II. EXPERIMENTAL METHODS AND CRYSTAL STRUCTURE

The ZFPMR spectra used in this work were taken at room temperature, 77, 4.2, and 2 K in the ZFPMR spectrometer previously described.[1] In each specific case below the microwave structure[1] used to record the spectrum will be given.

Ethylsulfate crystals used in this research were generally prepared according to the method of Erickson.[4] In the case of the deuterated ethylsulfates 99.7-at.%, Merck, Sharp, and Dohme Canada, Ltd. deuterium oxide was used not only for the reaction but also for washing the diethylsulfate. These samples were kept out of the atmosphere as much as possible to minimize isotopic exchange.

The bismuth magnesium double nitrate (BMDN) sample was prepared according to the method of Gerkin and Thorsell.[38] The magnesium used was Research Organic/Inorganic Chemical Corp. 99.99% magnesium-metal crystals. The bismuth used was Alfa Inorganics 99.99995% bismuth-metal shot. The nitric acid used was duPont reagent grade.

In the case of the isotopically enriched crystals for either of the above hosts, Union Carbide Oak Ridge National Laboratory stable isotope oxides were used. The $^{157}Gd_2O_3$ used was 99.7% in ^{157}Gd, 0.08% in ^{155}Gd, and the balance $I = 0$ isotopes. The ^{155}Gd used was 99.82% in ^{155}Gd, 0.07% in ^{157}Gd, and the balance $I = 0$ isotopes. The ^{160}Gd used was 99.99% in ^{160}Gd.

The lanthanide tris (ethylsulfate) nonahydrates are an isomorphic series of compounds, and as such have a special importance in the EPR of transition ions, especially the rare earths. The trivalent lanthanide ion, Ln^{3+}, may be any member of the rare-earth series and sits at a site of C_{3h} symmetry. The nine water molecules form a triangular prism, with the oxygens in the mirror plane at a greater distance from the threefold axis than the oxygens forming the end triangles. Good diagrams may be found in the crystal-structure papers of Ketelaar and Fitzwater and Rundle.[23] The water protons are *probably* hydrogen bonded to the oxygens of the sulfate groups, but have not been located experimentally. There are two formula units per unit cell, with approximately 18 nearest-neighbor sulfate oxygens about the lanthanide ion. The ethylsulfate anions are arranged in such a manner to make the space group $P6_3/m(C_{6h}^2)$. The waters of hydration may be replaced with D_2O when the crystal is synthesized, without deuteration of the ethylsulfate chains.

III. CRYSTAL FIELD

A. ^{160}Gd and natural gadolinium in $La(C_2H_5SO_4)_3 \cdot 9H_2O$

1. Results

ZFPMR spectra of gadolinium-doped LES where the gadolinium ions have either the naturally occurring isotopic composition or are 99.99% $^{160}Gd^{3+}$ ($I = 0$) are presented first. These studies were made for three reasons. First, it is necessary to ascertain if hyperfine structure from the two odd

isotopes can be observed superimposed on the $I=0$ lines when they are present in their natural composition of about 15% each. Second, accurate determination of ZFS is essential in order to test the adequacy of the spin-Hamiltonian formalism in zero field in a more stringent way than has been done in the past. Third, precisely determined crystal-field parameters must be used in the calculation of hyperfine-structure constants (see below).

The form of the spin Hamiltonian for the crystal field of C_{3h} symmetry has been well worked out.[13,17,39] Using a fictitious spin $\tilde{S}=\frac{7}{2}$ to represent the splitting in the ${}^8S_{7/2}$ ground state it is written in a form given by Elliott and Stevens[24] as

$$\mathcal{H}_{CF}=B_2^0\hat{O}_2^0+B_4^0\hat{O}_4^0+B_6^0\hat{O}_6^0+B_6^6\hat{O}_6^6 \qquad (3.1)$$

in which the B_l^m's are numerical constants, and the $\hat{O}_l^m$'s are Stevens's operator equivalents as have been extensively tabulated by Hutchings.[40]

This spin Hamiltonian leads to four distinct Kramers's doublets in zero field. If the small off-diagonal coefficient B_6^6 is neglected, their energies are given by

$$\begin{bmatrix}E_1\\E_2\\E_3\\E_4\end{bmatrix}=\begin{bmatrix}7&7&1\\1&-13&-5\\-3&-3&9\\-5&9&-5\end{bmatrix}\begin{bmatrix}b_2^0\\b_4^0\\b_6^0\end{bmatrix}=\begin{bmatrix}E(\pm\frac{7}{2})\\E(\pm\frac{5}{2})\\E(\pm\frac{3}{2})\\E(\pm\frac{1}{2})\end{bmatrix}, \qquad (3.2)$$

where $b_2^0=3B_2^0$, $b_4^0=60B_4^0$, $b_6^0=1260B_6^0$, and $b_6^6=1260B_6^6$, and M_S is the projection of $\tilde{S}$ on the crystal three-fold axis for the four states. Using simple $\Delta M_S=\pm 1$ selection rules, the three zero-field transitions are

$$\begin{bmatrix}E_1-E_2\\E_2-E_3\\E_3-E_4\end{bmatrix}=\begin{bmatrix}T_1\\T_2\\T_3\end{bmatrix}=\begin{bmatrix}6&20&6\\4&-10&-14\\2&-12&14\end{bmatrix}\begin{bmatrix}b_2^0\\b_4^0\\b_6^0\end{bmatrix},\quad \begin{aligned}I_1&=7\\I_2&=12\\I_3&=15\end{aligned} \qquad (3.3)$$

with approximate relative intensities as shown.

These three ZFPMR transitions are shown in Fig. 1. Their transition energies as a function of temperature are given in Table I. In order to determine the error in these transition frequencies, their positions have been measured as a function of modulation-field strength, in both resonant cavities and in traveling wave helices, and for ^{160}Gd as well as natural Gd. Standard deviations in transition frequencies are given in Table I. In each case transition frequencies for the fairly broad lines were picked as the midpoint of the full width at half-height of the transition. For a given transition this value may be picked with a precision several times greater than the standard deviation for the line position.

2. Discussion

It is appropriate to compare the present measurement of the ZFS with that obtained by other workers. The results of this comparison are given in Table I. We compare our directly measured ZFS with that of Dagg, Kemp, and Symmons[35] for two temperatures. The two sets of numbers agree within experimental error, primarily due to the large error limits of the other workers.

Present results may also be compared with zero-field transition frequencies predicted by variable-field EPR. The predicted frequencies are given for the high-field measurements of Dagg *et al.*, and for the low-field results of Gerkin and Thorsell.[38] In the former case, in order to obtain the error limit of the predicted frequency, the square root of the sum of the squares of the error limits on b_2^0, b_4^0, and b_6^0, as obtained from ordinary EPR, are multiplied by the squares of the matrix coefficients in Eq. (3.3) to convert them to errors in transition energies. The two sets of numbers thus obtained agree within the 0.3% experimental error. The uncertainty in the ZFPMR measurements is only slightly less than the uncertainty in the conventional EPR results. This is due to the linewidth in this salt (~25 MHz) and it is not a general statement about the relative precision of ZFPMR. In another salt with sharp lines, the fact that frequencies may easily be determined to about 1 ppm with ZFPMR, whereas fields may be measured to 100 ppm only with difficulty, would demonstrate the higher precision of ZFPMR.

TABLE I. Comparison of crystal field ($I=0$ isotopes) transition energies for gadolinium-doped lanthanum ethylsulfate at two temperatures.

	ZFPMR This work (measured)[a] (MHz)	ZFPMR Dagg *et al.* (measured)[b] (MHz)	EPR Dagg *et al.* (calc.)[b,c] (MHz)	Low-field EPR Gerkin & Thorsall (calc.)[d] (MHz)
4.2 K				
T_1	3383.0±2.1	3381.4±9	3381.4±2.8	...
T_2	2503.5±3.6	2500.3±25	2502.7±4.2	...
T_3	1371.9±3.9	1363.2±9	1366.2±3.9	...
77 K				
T_1	3446.6±2.1	3444.3±12	3444.0±2.8	3442.5±6
T_2	2550.4±3.6	2555.4±10.2	2549.1±4.2	2547.9±1.2
T_3	1396.8±3.9	1390.1±14.1	1391.0±3.9	1390.1±?[d]

[a]Error limits are taken as three standard deviations; hence $\sigma(T_1)=0.7$ MHz, $\sigma(T_2)=1.2$ MHz, and $\sigma(T_3)=1.3$ MHz.

[b]Error limits as given in their work (Ref. 35).

[c]Obtained from non-zero field measurements.

[d]In this work there is an unexplained 26.1-MHz splitting detected between $\Delta M_S=1$ and $\Delta M_S=-1$ transitions be a method of extrapolation from fields above 10 G. The frequency indicated here is the average of these two (Ref. 38).

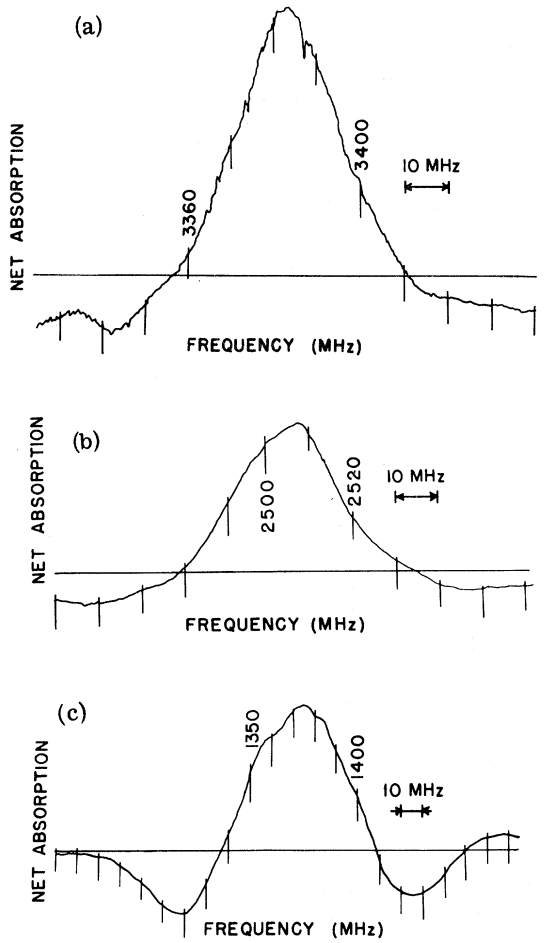

FIG. 1. ZFPMR spectrum of $La(C_2H_5SO_4)_3 \cdot 9H_2O$:0.1-mole% $^{160}Gd^{3+}$ at 4 K. Net absorption in arbitrary units is shown with net zero-field absorption directed up and net low-field absorption directed down. (a) T_1 transition $M_S = \pm\frac{5}{2} \rightarrow \pm\frac{7}{2}$. This spectrum was taken in a helix with 10-A modulation current and 10-μ Vlockin amplifier sensitivity. (b) T_2 transition $M_S = \pm\frac{3}{2} \rightarrow \pm\frac{5}{2}$. This spectrum was taken in a helix with 10-A modulation current and 50-μV lockin amplifier snnsitivity. (c) T_3 transition $M_S = \pm\frac{1}{2} \rightarrow \pm\frac{3}{2}$. This spectrum was taken in a cavity with 10-A modulation current and 100-μV lockin amplifier sensitivity. Under these conditions there is some overlap between zero and low-field absorption peaks. The true zero-field line shape is not completely resolved; hence, at this time it is premature to analyze the partially resolved fine structure of each line in terms of superhyperfine structure or other effects.

The low-field results of Gerkin and Thorsell are somewhat more problematical. These workers observed a 26.1-MHz splitting between the $\Delta M_S = 1$ and the $\Delta M_S = -1$ transition energies for T_3 by extrapolation from measurements taken above 10 G. Results from our measurements do not confirm the existence of these splittings. This additional complication may be the reason that the predicted frequencies from low-field EPR lie just outside the error limits of our measurements. The error limits used by these workers of less than 1 MHz may be somewhat optimistic.

For the treatment of hyperfine structure presented below, crystal-field parameters appropriate to these zero-field measurements will be necessary. This determination is not possible in closed form since, in C_{3h} symmetry, it is necessary to determine four crystal-field parameters with three zero-field transitions. This situation, however, becomes tractable because the b_6^6 coefficient is so small. If we use a typical value of -4.25×10^{-4} cm^{-1} as determined by Dagg *et al.*,[35] the coefficient $B_6^6 = 1.01 \times 10^{-2}$ MHz. The other three crystal-field coefficients may then be varied to fit exactly the three ZFS transitions. Neglect of the off-diagonal matrix elements connecting the $\pm\frac{7}{2}$ levels with the $\pm\frac{1}{2}$ levels via $\hat{O}_6^6$ leaves the best-fit crystal-field parameters invariant to about five significant figures. Indeed, second-order perturbation theory shows that this coefficient can lead to a position shift for the $\pm\frac{1}{2}$ or $\pm\frac{7}{2}$ energy levels of about 0.5 MHz, which is on the order of the standard deviation of transition frequencies. Considering the slow temperature dependence of B_6^6 (-0.01 kHz/K), the 77-K value is employed at both 77 and 4.2 K with little error. The best least-squares-fit crystal-field parameters are given in Table II.

The standard deviations in these parameters are derived from standard deviations in transition frequencies by taking the absolute value of the inverse of the matrix of coefficients in Eq. (3.3). The error is the square root of the sum of the squares of the terms obtained by multiplying this matrix by a column vector of standard deviations of transition frequencies. These are also given in Table II.

B. Natural gadolinium in various $Ln(C_2H_5SO_4)_3 \cdot 9D_2O$

1. Introduction and results

It has recently been pointed out by Gerkin and Thorsell[38] that crystals of $La(C_2H_5SO_4) \cdot 9D_2O$ show a Gd^{3+} linewidth up to a factor of 2 less than the corresponding hydrate. They therefore used such crystals in place of hydrated crystals in their low-field EPR studies of Gd^{3+} in LES. It is not obvious from ordinary EPR or even low-field EPR, but it is immediately apparent from ZFPMR that *the crystal-field parameters for the deuterate are different from those of the hydrate*. This difference is immediately obvious using ZFPMR, since one measures the ZFS directly without recourse to computations based on variable-field data.

Inasmuch as the origin of crystal-field splitting of Gd^{3+} is still an open question, it becomes important to pursue the nature of this deuteration effect on the crystal parameters. Accordingly, both

TABLE II. Best least-squares-fit cyrstal-field spin-Hamiltonian parameters for $^{160}Gd^{3+}$-doped LES at two temperatures, using $b_6^6 = -4.25\times10^{-4}$ cm^{-1}.

Coefficient	Temp. (K)	Value (MHz)	Std. dev. (MHz)[a]	Value (10^{-4} cm^{-1})	Std. dev. (10^{-4} cm^{-1})
B_2^0	77	204.418		6.187	
	4	200.668	0.083	66.936	0.027
B_4^0	77	−0.2028		-6.765×10^{-2}	
	4	−0.1996	0.0013	-6.656×10^{-2}	0.043×10^{-2}
B_6^0	77	1.376×10^{-3}		4.59×10^{-4}	
	4	1.373×10^{-3}	0.072×10^{-3}	4.58×10^{-4}	0.24×10^{-4}
b_2^0	77	613.25		204.560	
	4	602.01	0.25	200.807	0.083
b_4^0	77	−12.168		−4.059	
	4	−11.973	0.077	−3.994	0.026
b_6^0	77	1.734		0.578	
	4	1.730	0.091	0.577	0.030
rms error of least-square fit	77	6.0×10^{-4}	...		...
	4		...		...

[a]Standard deviations are taken to be the same at both temperatures.

temperature and host (La, Sm, Er) ionic-radius dependence of crystal-field parameters for the deuterate were investigated.

The temperature dependence of ZFS in ethylsulfate hydrates has been discussed by several workers.[17,35,37] Dagg, Kemp, and Symmons[35] noted that ZFS is a maximum at about 130 K in LES. Between 77 and 4 K the ZFS is, within experimental error, linearly dependent on absolute temperature. The dependence on temperature from 290 to 77 K for several lanthanide ethylsulfates has also been studied by Gerkin and Thorsell.[37]

To compare deuterate with hydrate in this regard we have studied the lanthanum salt at 77 and 4 K. The results are given in Tables III and IV in which deuterate data may be compared with the corresponding hydrate data. It is immediately obvious from Table IV that the temperature dependence of each is the same. This dependence probably indicates that the gross features of hydrogen bonding in each are quite similar.

ZFS and crystal-field parameters for several deuterated lanthanide ethylsulfates at 77 K have also been studied. The results may be found in Table V. The dependence of b_2^0 on the ionic radius of the host lanthanide ion at both 77 K and room temperature is linear. Figure 2 presents the dependence of b_2^0 on the radii for hydrate and deuterate. Both are seen to be linear, with best weighted-least-squares slopes of 288.9×10^{-4} cm^{-1} Å^{-1} for the hydrate and 295.6×10^{-4} cm^{-1} Å^{-1} for the deuterate, at 77 K. Considering the errors in b_2^0 values and the fact that only three points were used to determine the slope, we judge these two slopes to agree within experimental error.

2. Discussion

It has been shown that within experimental error the deuterate and hydrate crystal fields depend in the same way on temperature and host lanthanide ion radius. We wish to inquire, then, what causes the deuterate to have a 4% stronger quadrupolar crystal-field parameter b_2^0. The deuteron differs from the proton in three fundamental ways. First,

TABLE III. Crystal-field parameters and ZFS for LES hydrate and LES deuterate at two temperatures. In each case b_6^6 was taken as 0. The error limits are three standard deviations.

	Temp. (K)	Hydrate	Deuterate
T_1 (MHz)	77	3446.6±2.1	3598±4
	4	3383.0±2.1	3531.0±4
T_2(MHz)	77	2550.4±3.6	2645±4
	4	2503.5±3.6	2597.7±4
T_3 (MHz)	77	1396.8±3.9	1440.5±10
	4	1371.9±3.9	1413.0±10
b_4^0 (10^{-4} cm^{-1})	77	204.56±0.15	212.64±0.26
	4	200.81±0.15	208.73±0.26
b_4^0 (10^{-4} cm^{-1})	77	−4.06±0.05	−3.95±0.10
	4	−3.99±0.05	−3.88±0.10
b_6^0 (10^{-4} cm^{-1})	77	0.58±0.06	0.56±0.13
	4	0.58±0.06	0.52±0.13

TABLE IV. Temperature dependence of crystal-field parameters and ZFS for LES hydrate and LES deuterate in the region from 77 to 4 K. All dependences have been assumed linear. The error limits given are about three standard deviations.

	Hydrate	Deuterate
$\frac{dT_1}{dT}$ (MHz K^{-1})	0.87 ± 0.06	0.92 ± 0.11
$\frac{dT_2}{dT}$ (MHz K^{-1})	0.64 ± 0.10	0.65 ± 0.11
$\frac{dT_3}{dT}$ (MHz K^{-1})	0.34 ± 0.11	0.38 ± 0.27
$\frac{db_2^0}{dT}$ (10^{-4} cm^{-1} K^{-1})	0.051 ± 0.004	0.053 ± 0.007
$\frac{db_4^0}{dT}$ (10^{-4} cm^{-1} K^{-1})	-9.59×10^{-4} $\pm 1.4\times10^{-3}$	-9.59×10^{-4} $\pm 2.8\times10^{-3}$
$\frac{db_6^0}{dT}$ (10^{-4} cm^{-1} K^{-1})	$0 \pm 1.6\times10^{-3}$	5.5×10^{-4} $\pm 3.6\times10^{-3}$

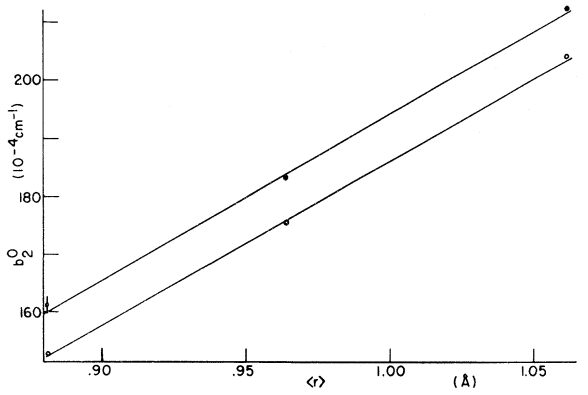

FIG. 2. Quadrupolar-crystal-field coefficient b_2^0 for three Gd^{3+}-doped lanthanide ethyl sulfates vs $4f$-electron radii. The open circles are for $Ln(C_2H_5SO_4)_3 \cdot 9D_2O$. The average $4f$ radii are those estimated by Templeton and Dauben (Ref. 41), and correspond to Er^{3+}, Sm^{3+}, and La^{3+}. The crystal-field parameters are from Table V. The experimental error is smaller than the circle size except in the case of the erbium deuterate.

the magnetic moment of the deuteron is a factor of 3.25 times smaller than the proton. Second, the deuteron is a spin-one particle and thus has a small quadrupole moment. Third, the deuteron mass is a factor of 2 greater than that of the proton. Considering the smallness of the quadrupole moment and the electrostatic nature of crystal-field theory, a mechanism based on the first two differences would be unlikely. The third difference, however, leads not only to a change in vibrational frequency, but also to a change in the potential in which the hydrogen-bonded proton or deuteron vibrates (see, for example, Hamilton and Ibers[42]). The hydrogen bond length or angle could change.

Protons or deuterons on the waters of hydration are almost surely hydrogen bonded to oxygens on the sulfate groups.[23b] While evidence is not conclusive, it is usually suggested that electric-dipole moments of the water molecules are aligned with negative end toward the lanthanide ion. Hence the nearest neighbors of the central Ln^{3+} ion are oxygens, with hydrogens pointing toward the negative sulfate groups. A lengthening of the hydrogen bond on deuteration might cause not only a change in the lattice constant but also a change in the metal-oxygen distance. Indeed, this system is particularly interesting from the point of view of crystal-field theory since the ligands are neutral. Such a rearrangement in the hydrogen bonding on deuteration would produce a change in the static crystal field. If this small change in structure could be observed experimentally it might then be possible to correlate it with the observed change in crystal-field parameters upon deuteration.

If the Gd-O distance does in fact change, this

TABLE V. Crystal parameters and ZFS for three lanthanide ethylsulfate hydrates and deuterates at 77 K with their standard deviations. The calculations assume $b_6^6 = 0$. The hydrate data are from Ref. 37.

	Lanthanum ethylsulfate		Samarium ethylsulfate		Erbium ethylsulfate	
	Hydrate	Deuterate	Hydrate	Deuterate	Hydrate	Deuterate
T_1 (MHz)	3440.7 ± 1.9	3598.0 ± 3	2525.7 ± 2.6	3080.5 ± 2	2515.1 ± 6.1	2685 ± 25
T_2 (MHz)	2547.5 ± 1.4	2645 ± 3	2202.4 ± 1.7	2301 ± 2	1927.9 ± 4.4	2055 ± 25
T_3 (MHz)	1390.2 ± 1.2	1440.5 ± 10	1218.7 ± 1.5	1231.7 ± 5	1084.4 ± 3.8	1075 ± 50
b_2^0 (10^{-4} cm^{-1})	204.17 ± 0.08	212.64 ± 0.24	175.49 ± 0.10	183.18 ± 0.13	152.69 ± 0.24	161.26 ± 1.45
b_4^0 (10^{-4} cm^{-1})	-4.02 ± 0.02	-3.95 ± 0.10	-4.01 ± 0.03	-3.60 ± 0.05	-4.03 ± 0.07	-3.48 ± 0.55
b_6^0 (10^{-4} cm^{-1})	0.51 ± 0.02	0.56 ± 0.13	0.53 ± 0.02	0.088 ± 0.07	0.57 ± 0.06	-0.40 ± 0.68

would have important consequences for diffraction crystalography. It is customary in x-ray or neutron-diffraction studies to hold the metal-oxygen distance constant when simultaneously refining the structure for protonated and deuterated species.[43,44] By this simple mechanism, the effect of deuteration might be the same as a change in lattice size with temperature or hydrostatic pressure.[45,46]

Even if the Gd-O distance does not change, it is possible that the positions of the deuterons do. It is known that the water hydrogens are close enough to the gadolinium ion to allow dynamic nuclear-polarization experiments to be performed.[36] In *ab initio* calculation of crystal-field parameters by lattice summations, results are quite sensitive to how the water dipole moment is treated.[47] Generally, it is accommodated by assuming that the water molecule is composed of fractional charges placed so the entire molecule is neutral. Clearly, a change in the water bond angle would cause b_2^0 to change. Less-accurate calculations include the nearest-neighbor oxygens only, predicting no effect for a change in hydrogen-bond orientation.

If equilibrium positions of neither oxygens nor hydrogens change when the structure for the hydrate and deuterate are refined independently, one might have to resort to a dynamic crystal-field theory to account for the difference by considering a change in the oxygen-hydrogen vibration frequency.

Measurement of the dependence of the nuclear-quadrupole-coupling parameter on deuteration, host lattice, and hydrostatic pressure would yield information on the contribution of the lattice or crystal electric-field gradient eq_c to the total field gradient. A change due to these effects would be difficult to see for the deuterate in LES because its magnitude would be about the same size as the presently available standard deviation of P, due to linewidth.

IV. HYPERFINE SPECTRA OF ^{155}Gd AND ^{157}Gd

A. Results and analysis

Hyperfine structure was not resolved in the naturally occurring gadolinium spectra. In order to determine whether it was really absent, or measure its magnitude if present, isotopically enriched crystals of 0.1-mole% concentration were prepared. Since g is isotropic to five decimal places,[39b] the hyperfine-structure Hamiltonian in axial symmetry may be represented as[13]

$$\mathcal{H}_{\rm hfs} = A\hat{S}_z\hat{I}_z + \tfrac{1}{2}A(\hat{S}_+\hat{I}_- + \hat{S}_-\hat{I}_+) + P[\hat{I}_z^2 - \tfrac{1}{3}I(I+1)]\,, \tag{4.1}$$

in which A is the isotropic hyperfine constant, and P is the nuclear-electric-quadrupole constant, and $\hat{I}$ is the nuclear-spin operator. For these isotopes $I=\frac{3}{2}$ and as before $\tilde{S}=\frac{7}{2}$. The Hamiltonian, therefore, is a 32×32 matrix when represented in the complete set of high-field states, $|M_S M_I\rangle = |M_S\rangle|M_I\rangle$ quantized along the three-fold crystal symmetry axis.

In order to obtain an approximate analysis of the zero-field spectra, it would be very useful to have approximate analytical expressions for the zero-field energy levels. It was shown above that the off-diagonal term in the crystal field is quite small, so it will be temporarily neglected. Zero-field states can then be treated as pure high-field states $|M_S M_I\rangle$. For convenience, elements off diagonal in the hyperfine operator if $M_S \neq \pm\frac{1}{2}$ will also be neglected. This approximation is worse than the neglect of off-diagonal crystal-field terms, but it will be adequate for an approximate set of hyperfine constants from which to initiate a least-squares analysis of the exact diagonalization of the full 32×32 matrix. These off-diagonal elements cause shifts on the order of 3.5 MHz. Under these two approximations the matrix breaks up into submatricies of size no greater than 2×2. The energy-level formulas are given in Table VI. Using $\Delta M_S = \pm1$, $\Delta M_I = 0$ selection rules one may then calculate the spectrum. A 15-line spectrum is predicted, with crystal-field transition T_1 splitting

TABLE VI. Approximate hyperfine energy levels for $S=\frac{7}{2}$ and $I=\frac{3}{2}$ [$R \equiv (\frac{49}{4}A^2 - AP + P^2)^{1/2}$].

Levels	Energies	Kets in eigenfunction
E_{41}	$\frac{3}{4}A+P+E_4$	$\|\frac{1}{2}\ \frac{3}{2}\rangle,\ \|-\frac{1}{2}-\frac{3}{2}\rangle$
E_{42}	$\frac{15}{4}A-P+E_4$	$\|\frac{1}{2}-\frac{1}{2}\rangle,\ \|-\frac{1}{2}\ \frac{1}{2}\rangle$
E_{43}	$-\frac{17}{4}A-P+E_4$	$\|\frac{1}{2}-\frac{1}{2}\rangle,\ \|-\frac{1}{2}\ \frac{1}{2}\rangle$
E_{44}	$-\frac{1}{4}A+R+E_4$	$\|\frac{1}{2}\ \frac{1}{2}\rangle,\ \|-\frac{1}{2}\ \frac{3}{2}\rangle$ $\|\frac{1}{2}-\frac{3}{2}\rangle,\ \|-\frac{1}{2}-\frac{1}{2}\rangle$
E_{45}	$-\frac{1}{4}A-R+E_4$	$\|\frac{1}{2}\ \frac{1}{2}\rangle,\ \|-\frac{1}{2}\ \frac{3}{2}\rangle$ $\|\frac{1}{2}-\frac{3}{2}\rangle,\ \|-\frac{1}{2}-\frac{1}{2}\rangle$
E_{31}	$\frac{9}{4}A+P+E_3$	$\|\frac{3}{2}\ \frac{3}{2}\rangle,\ \|-\frac{3}{2}-\frac{3}{2}\rangle$
E_{32}	$\frac{3}{4}A-P+E_3$	$\|\frac{3}{2}\ \frac{1}{2}\rangle,\ \|-\frac{3}{2}-\frac{1}{2}\rangle$
E_{33}	$-\frac{3}{4}A-P+E_3$	$\|\frac{3}{2}-\frac{1}{2}\rangle,\ \|-\frac{3}{2}\ \frac{1}{2}\rangle$
E_{34}	$-\frac{9}{4}A+P+E_3$	$\|\frac{3}{2}-\frac{3}{2}\rangle,\ \|-\frac{3}{2}\ \frac{3}{2}\rangle$
E_{21}	$\frac{15}{4}A+P+E_2$	$\|\frac{5}{2}\ \frac{3}{2}\rangle,\ \|-\frac{5}{2}-\frac{3}{2}\rangle$
E_{22}	$\frac{5}{4}A-P+E_2$	$\|\frac{5}{2}\ \frac{1}{2}\rangle,\ \|-\frac{5}{2}-\frac{1}{2}\rangle$
E_{23}	$-\frac{5}{4}A-P+E_2$	$\|\frac{5}{2}-\frac{1}{2}\rangle,\ \|-\frac{5}{2}\ \frac{1}{2}\rangle$
E_{24}	$-\frac{15}{4}A+P+E_2$	$\|\frac{5}{2}-\frac{3}{2}\rangle,\ \|-\frac{5}{2}\ \frac{3}{2}\rangle$
E_{11}	$\frac{21}{4}A+P+E_1$	$\|\frac{7}{2}\ \frac{3}{2}\rangle,\ \|-\frac{7}{2}-\frac{3}{2}\rangle$
E_{12}	$\frac{7}{4}A-P+E_1$	$\|\frac{7}{2}\ \frac{1}{2}\rangle,\ \|-\frac{7}{2}-\frac{1}{2}\rangle$
E_{13}	$-\frac{7}{4}A-P+E_1$	$\|\frac{7}{2}-\frac{1}{2}\rangle,\ \|-\frac{7}{2}\ \frac{1}{2}\rangle$
E_{14}	$-\frac{21}{4}A+P+E_1$	$\|\frac{7}{2}-\frac{3}{2}\rangle,\ \|-\frac{7}{2}\ \frac{3}{2}\rangle$

TABLE VII. Hyperfine transitions for $S=\frac{7}{2}$, $I=\frac{3}{2}$ according to a $\Delta M_S=\pm 1$, $\Delta M_I=I$ selection rule. The energy level formulas are from Table VI. The first subscript of a T_{mn} indicates from which crystal-field transition it is derived.

T_1	
$T_{11}\equiv E_{11}-E_{21}=T_1+\frac{3}{2}A$	$T_{12}\equiv E_{12}-E_{22}=T_1+\frac{1}{2}A$
$T_{13}\equiv E_{13}-E_{23}=T_1-\frac{1}{2}A$	$T_{14}\equiv E_{14}-E_{24}=T_1-\frac{3}{2}A$
T_2	
$T_{21}\equiv E_{21}-E_{31}=T_2+\frac{3}{2}A$	$T_{22}\equiv E_{22}-E_{32}=T_2+\frac{1}{2}A$
$T_{23}\equiv E_{23}-E_{33}=T_2-\frac{1}{2}A$	$T_{24}\equiv E_{24}-E_{34}=T_2-\frac{3}{2}A$
T_3	
$T_{31}\equiv E_{33}-E_{43}=T_3+\frac{7}{2}A$	$T_{32}\equiv E_{32}-E_{44}=T_3+A-P-R$
$T_{33}\equiv E_{32}-E_{45}=T_3+A-P+R$	$T_{34}\equiv E_{31}-E_{41}=T_3+\frac{3}{2}A$
$T_{35}\equiv E_{34}-E_{44}=T_3-2A+P-R$	$T_{36}\equiv E_{34}-E_{45}=T_3-2A+P+R$
$T_{37}\equiv E_{33}-E_{42}=T_3-\frac{9}{2}A$	

into four lines numbered T_{11} to T_{14}, transition T_2 splitting into four lines numbered T_{21} to T_{24}, and transition T_3 splitting into seven lines numbered T_{31} to T_{37}. The transition energies are given in Table VII.

Of course, the ordering of these transitions in energy will depend on the signs and magnitudes of the parameters. One may easily see that T_1 and T_2 are each split by the same amount and consist of four equally spaced lines, each with a total spread of $3A$. Their positions are independent of P to this order of approximation and the spectrum is invariant to the sign of A. It is therefore necessary to look to the T_3 transition splitting to determine P and the sign of A and P. Note that the splitting is asymmetrical about T_3 and hence the absolute and relative signs of A and P may be determined (see Table VII). As previously mentioned, Bleaney *et al.*[25] were able to determine the absolute signs of the crystal-field parameters; absolute signs are thereby obtained for *all diagonal* parameters in the spin-Hamiltonian (A, P, B_l^0).

Figure 3 presents spectra for ^{157}Gd-doped LES at 4 K. It is obvious that the hyperfine splitting is not resolved for T_1 and T_2. There are, however, five lines present for T_3. In order to assign the lines, the approximate expressions of Table VII are needed. A series of plots of these expressions for T_{3n} can be computed for a wide range of values of A and P. Each such plot is for P ranging from -100 to 100 MHz for constant A, such as is illustrated in Fig. 4 for $A=18$ MHz. On examining such plots for A ranging from -25 to 25 MHz, only one set of approximate values fits the observed spectra for each isotope and different modulation strengths. The assignment, then, of the five-line spectrum is as follows. The broad center line is assumed to

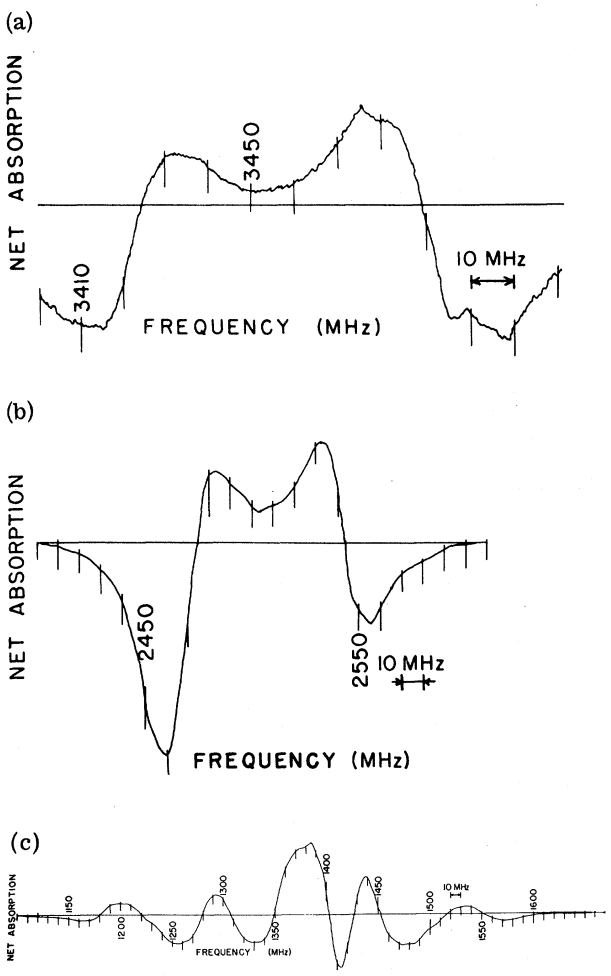

FIG. 3. ZFPMR spectrum of $La(C_2H_5SO_4)\cdot 9H_2O$: 0.1-mole% $^{157}Gd^{3+}$. Net absorption in arbitrary units is shown with net zero-field absorption directed up and net low-field absorption directed down. (a) T_{1n} transition corresponding to the hyperfine splitting of the $I=0$ T_1 transition. This spectrum was taken at 77 K in a cavity with 1-A modulation current and 2-μV lockin amplifier sensitivity. (b) T_{2n} transition corresponding to the hyperfine splitting of the $I=0$ T_2 transition. This spectrum was taken at 4 K in a cavity with 500-mA modulation current and 10 μV lockin amplifier sensitivity. (c) T_{3n} transition corresponding to the hyperfine splitting of the $I=0$ T_3 transition. This spectrum was taken at 4 K in a cavity with 1-A modulation current and 50-μV lockin amplifier sensitivty.

consist of three unresolved transitions. The remaining four lines are assigned as T_{35}, T_{37}, T_{31}, and T_{33}, in order of increasing frequency. The transition frequencies for the four lines which are invariant to modulation-field intensity, are given in Table VIII.

Least-squares best-fit parameters are calculated by numerical diagonalization of the 32×32 Hamiltonian matrix *with all off-diagonal elements included.*

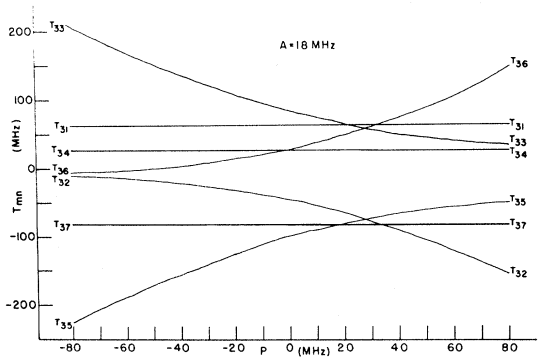

FIG. 4. Approximate ZFPMR hyperfine T_{1n} transition energies as a function of the nuclear-electric-quadrupole spin-Hamiltonian parameter P for constant nuclear-magnetic-dipole spin-Hamiltonian parameter $A = 18$ MHz. The formulas for the T_{1n} are from Table VII.

The best-fit crystal-field parameters from ^{160}Gd, as determined in the *previous* Sec. III, are employed. Any possible isotopic dependence of the crystal-field parameters (for Gd isotope) is thereby neglected. Such a dependence has been proposed by Marshall[48] for Gd^{3+} in charge-compensated ThO_2, but the difference between the $I = 0$ isotope and the odd isotopes is just larger than his experimental error. Since our lines are much broader than those in ThO_2, any such effects are unlikely to be observed in this system.

The rms error in the fit is defined as δ and is also given in Table VIII. After the least-squares routine has converged on a minimum δ, there are various sets of local minima which give approximately the same minimum value, due to roundoff error in the computation. A final value for A and P may then be taken as the average of those belonging to the local minima. The standard deviation of these local minima average of δ, A, and P is defined as $\sigma_f[\delta]$, $\sigma_f[A]$, and $\sigma_f[P]$, respectively. Values of A and P so calculated are given in Table IX. Predicted transition frequencies from them and the values of δ and the σ_f's are given in Table VIII. Note that in three of the four cases, the rms error in calculated frequency for each transition is greater than the standard deviation of frequency measurements (2 MHz at 77 K, 1.2 MHz at 4 K). Note also that the observed frequencies at 77 K are always higher than the calculated ones. One could reduce δ for these cases by lowering the value of T_3; however, there is no justification for changing experimental values in this manner, so the small systematic error in calculated frequencies must simply be accepted.

In order to calculate the standard deviations in parameters A and P, local linear approximations to the derivitives of the transition frequencies with respect to A and P are used. These standard deviations in parameters $\sigma[A]$ and $\sigma[P]$ are propagated directly from the standard deviations in observed transition frequencies. The standard deviations thus calculated appear in Table IX. For some calculations involving both A and P it may be necessary to calculate the error in a resultant function. This computation requires the covariance of A and P as well as their standard deviations, and this covariance is estimated to be 1.56×10^{-1} MHz at 77 K and 1.26×10^{-1} MHz at 4 K. A description of the statistical procedures may be found in a recent monograph.[49] Of course $\sigma_f[A]$ and $\sigma_f[P]$ are much smaller than $\sigma[A]$ and $\sigma[P]$, as would be expected. It should be emphasized that the standard deviations quoted here are indicative of the linewidth of Gd^{3+} in this salt, rather than indicative of the accuracy of ZFPMR.

Having determined least-squares best-fit hyperfine constants, it is of interest to determine, in a qualitative way, the fit of the relative intensities. This is a complicated problem in ZFPMR because of the influence of the modulation magnetic field. Since the modulation magnetic field may vary over the sample volume, the line-shape parameters for the low-field spectrum may be different than for the zero-field spectrum. While it has been demonstrated that such factors play little or no role in the determination of zero-field transition frequencies,[10] the over-all shape and appearance of the

TABLE VIII. Transition frequencies and other parameters for gadolinium-doped lanthanum ethylsulfate at two temperatures for best least-squares-fit hyperfine parameters.

		^{157}Gd		^{155}Gd	
Parameter	(MHz)	77 K	4 K	77 K	4 K
T_{35}	obs.[a]	1225.0	1200.4	1248.6	1219.4
	calc.	1222.5	1200.8	1248.0	1219.6
T_{37}	obs.[a]	1320.2	1296.0	1334.6	1310.9
	calc.	1315.0	1293.4	1332.0	1309.4
T_{31}	obs.[a]	1465.9	1440.4	1451.2	1425.3
	calc.	1460.5	1438.0	1448.5	1423.9
T_{33}	obs.[a]	1557.9	1532.8	1535.2	1514.8
	calc.	1553.0	1533.5	1534.0	1515.1
δ[b]		4.3	1.6	1.8	0.9
$\sigma[\delta]$[c]		5.2×10^{-3}	9.9×10^{-5}	2.5×10^{-3}	3.9×10^{-3}
$\sigma_f[A]$[d]		5.1×10^{-2}	7.7×10^{-3}	2.6×10^{-2}	6.8×10^{-3}
$\sigma_f[P]$[e]		1.4×10^{-1}	4.4×10^{-2}	5.3×10^{-2}	4.1×10^{-2}

[a]The standard deviation of transition frequencies is taken to be 2.0 MHz at 77 K, and 1.2 MHz at 4 K.

[b]The rms error of the fit.

[c]The standard deviation of the rms error of the fit. This is caused by roundoff error in the calculation. Several sets of A and P give rise to approximately the same δ in the local minimum.

[d]The standard deviation of these A values described in footnote c. The best fit A is the mean of these A values.

[e]The standard deviation of the various P values described in footnote c. The best fit P is the mean of these P values.

TABLE IX. Best-fit hyperfine constants at two temperatures. For definition of symbols, see text.

Isotope	Temp. (K)	A	$\sigma[A]$[a]	P	$\sigma[P]$[a]	Units[b]
^{157}GD	77	18.26	0.37	−52.86	1.26	MHz
^{157}Gd	4	18.10	0.22	−53.09	0.76	MHz
^{155}Gd	77	14.59	0.37	−48.01	1.26	MHz
^{155}Gd	4	14.33	0.22	−51.16	0.76	MHz
^{157}Gd	77	6.09	0.12	−17.63	0.42	10^{-4} cm^{-1}
^{157}Gd	4	6.034	0.07	−17.71	0.25	10^{-4} cm^{-1}
^{155}Gd	77	4.86	0.12	−16.01	0.42	10^{-4} cm^{-1}
^{155}Gd	4	4.78	0.07	−17.06	0.25	10^{-4} cm^{-1}
^{157}Gd	77	6.55	0.13	−18.96	0.45	G
^{157}Gd	4	6.49	0.08	−19.04	0.27	G
^{155}Gd	77	5.23	0.13	−17.22	0.45	G
^{155}Gd	4	5.14	0.08	−18.35	0.27	G

[a]Based on an averaged standard deviation of 2 MHz for transition frequencies at 77 K, and 1.2 MHz at 4 K.

[b]Conversion of MHz to G was accomplished using a g factor of 1.9919 [Ref. 39(a)].

spectra vary greatly with modulation-field strength. The most stringent test of the quality of calculated parameters is thus a complete synthesis of observed total spectrometer output. Therefore, many calculated spectra have been plotted assuming various effective modulation fields and various Gaussian linewidths for the zero- and low-field spectra. A typical result is shown in Fig. 5(a). While the fit is qualitatively correct in many respects, it is not an exact fit (compare with Fig. 3). Of course, spectra for low fields may depend on the angles between modulation field and crystal axes, and, as such, on whether single crystals were used. To illustrate the angular effect, Fig. 5(b) contains a spectrum with the modulation field perpendicular to the crystal axis. It is clear that for an exact computation of the spectrum would have to integrate over the entire sample volume to account for the field magnitude and angular variations.

Approximate expressions for transition energies indicated that T_1 and T_2 should each be split into four equally spaced lines with total spread 3A. The theoretical line-shape calculations show that observed spectra do not contradict this conclusion. Indeed, starting with the best fit A, one may calculate the spectrum shown in Fig. 5(c), after suitable choice of line shapes. The "doublet" spectrum arises from the large linewidth in this salt.

It is particularly interesting to examine a salt with sharper lines but still characterized by a similar Hamiltonian. The expected zero-field spectrum for $Bi_2Mg_3(NO_3)_{12}\cdot 24H_2O$, bismuth magnesium double-nitrate (BMDN), is very similar, even though the symmetry is approximately C_{3i} (exactly C_3) rather than C_{3h}.[50–53] The corresponding hyperfine split T_2 transition is shown in Fig. 6. Total spread in the spectrum is consistent with recent ENDOR measurement of the hyperfine constants of this sample by Butti *et al.*[54] The T_3

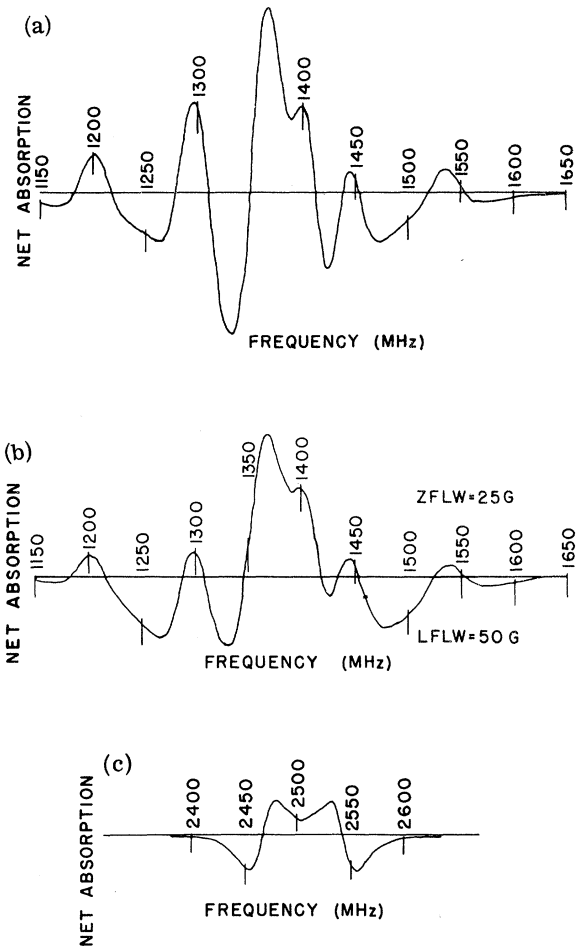

FIG. 5. Computer-synthesized ZFPMR spectra of Gd^{3+}-doped $La(C_2H_5SO_4)_3\cdot 9H_2O$ at 4 K, using the best least-squares fit spin-Hamiltonian parameters. Net absorption in arbitrary units is shown with net zero-field absorption directed up and net low-field absorption directed down. Effective conditions were chosen to give qualitative agreement with line intensity and shape. (a) T_{1n} transitions at an effective modulation field of 5 G directed parallel to the crystal-symmetry axis. The effective zero-field linewidth is 25 G and the effective low-field linewidth is 60 G. Compare with Fig. 3(c). (b) T_{1n} transitions at an effective modulation field of 10 G directed perpendicular to the crystal symmetry axis. The effective zero-field linewidth is 25 G and the effective low-field linewidth is 50 G. Compare with Fig. 3(c). (c) T_{2n} transitions at an effective modulation field of 5 G directed parallel to the crystal symmetry axis. The effective zero-field linewidth is 20 G and the effective low-field linewidth is 40 G. Compare with Fig. 3(b).

transition, from which a measurement of the quadrupole parameter P could be made, lies at about 750 MHz. The recent availability of crystal-field parameters for a variety of gadolinium-doped lanthanide double nitrates[55] (LMDN) makes it particularly interesting to determine the series varia-

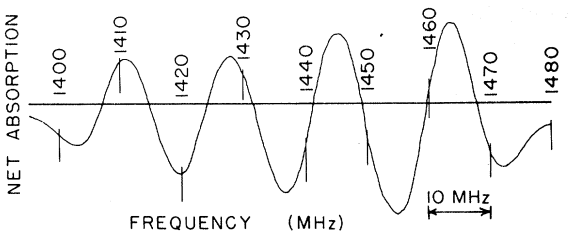

FIG. 6. ZFPMR spectrum of the T_{2n} transition corresponding to the hyperfine splitting of the T_2 transition of $Bi_2Mg_3(NO_3)_{12}\cdot 24H_2O$:0.1-mole% $^{157}Gd^{3+}$ at 4 K. Net absorption in arbitrary units is shown with net zero-field absorption directed up and net low-field absorption directed down. This spectrum was taken in a cavity with 500-mA modulation current and 20-μV lockin amplifier sensitivity. Compare with Fig. 3(b) in which the lines are broader.

tion of the hyperfine constants by ZFPMR or zero-field electron nucleus double resonance (ZFENDOR).

B. Discussion

Hyperfine structure (hfs) for Gd^{3+} is governed by properties of the half-filled $4f$ shell. The $^8S_{7/2}$ ground state arising from the $4f^7$ configuration is almost pure, since the next-higher electronic state $^6P_{7/2}$ is from the same configuration and has an energy of about 32 000 cm^{-1}. Wybourne[19] estimates the coefficient for mixing $^6P_{7/2}$ into the ground state in intermediate coupling to be about 0.1618 from the g values for the states. It is reasonable, therefore, to begin our discussion of hyperfine structure from the assumption of pure $^8S_{7/2}$.

1. Magnetic-dipole hyperfine structure

There are three basic contributions to the "magnetic-dipole hyperfine" structure. They are the orbital, spin-dipolar, and Fermi contact interactions.[56] For a half-filled shell in LS coupling, all three contributions vanish. The first vanishes because there is no orbital angular momentum, the second vanishes because spherical symmetry of the electron spin magnetization gives rise to no net magnetization at the nucleus, and the third vanishes because f electrons have a node at the origin.

Appearance, then, of hfs in a half-filled shell or S-state ion is ascribed to breakdown of these assumptions due to one or more of several mechanisms. One such mechanism is core polarization.[12,13] In order to calculate the magnitude of core polarization one must do a so-called unrestricted Hartree-Fock calculation,[57] in which two electrons in the same orbital are allowed to have different radii, depending on the orientation of their spins with respect to the open shell electrons.

A second possible contribution to S-state ion hyperfine interactions is relativistic in nature and deals with breakdown of LS coupling. This contribution, denoted A_{BDLSC} in the notation of Sandars and Beck,[56e] is due to mixing of higher electronic states into the ground state by spin-orbit and spin-spin interactions. This has the effect of destroying spherical symmetry for the half-filled and closed shells and thus some f or other $l\neq 0$ electrons can appear at the origin. For the $^8S_{7/2}$ state of europium these authors find the spin-orbit operator dominant. A_{BDLSC} is found to be opposite in sign to the experimental A and "the Casimir effect" must be used to bring the calculated value of A closer to the experimental one. In order to estimate the value of $A_{Cas.}$ one must numerically solve the radial Dirac equation. Even by using the best relativistic wave functions for europium available at the time, they can reduce the discrepancy between A_{BDLSC} and experiment by only one-half.

Fortunately, there is an experimental way to tell whether core polarization or relativistic effects give rise to A for half-filled shell ions. One may define the so called hyperfine anomaly Δ which is given by the equation

$$^{155}A/^{157}A=[g_n(155)/g_n(157)](1+\Delta)\ , \qquad (4.2)$$

in which the g_n's are the nuclear g values for the indicated isotopes. Δ is essentially a measure of how the distribution of nuclear magnetization inside the nucleus differs for each isotope. This isotope effect on the nuclear-magnetization distribution is probed through interaction with s electrons inside the nucleus. Our interest is not necessarily in nuclear physics, but rather in the fact that core polarization will lead to a hyperfine anomaly and relativistic effects will not.[58]

Table X presents a survey of measurements of A and calculated Δ's for Gd^{3+} in a variety of hosts. Included is our measurement of A in LES, which is the largest value for Gd^{3+} in a diamagnetic host. The hyperfine-structure anomalies are calculated using a ratio of g_n values of 0.7633 ± 0.0035 from electron-nucleus double resonance (ENDOR)[59] in CeO_2. It is seen that Δ is zero within experimental error for diamagnetic hosts even for precise ENDOR determinations. Large errors in Δ are primarily due to error in the g_n ratio; hence, ENDOR determinations show little improvement in accuracy over EPR determinations. Improvement in the accuracy of Δ must await a better measurement of the ratio of the g_n's.

One can ask whether the upper bound on Δ, set by its experimental error, is small enough to decide that core polarization is not playing a major role in the appearance of hyperfine structure. The hfs anomaly for Eu^{2+} was determined by Baker and Williams[60] to be $(-0.78\pm 0.11)\%$, in a situation for which it has been suggested that core polarization accounts for about 80% of the hyperfine constant. One must therefore conclude that present error

TABLE X. Magnetic dipolar hyperfine constants for gadolinium as determined by EPR, ENDOR, and other techniques.[a]

Material and technique	Ref.[b]	Temp. (K)	^{157}A (MHz)	^{155}A (MHz)	$^{155}A/^{157}A$	$-\Delta$[c](%)
ThO_2	1	290	15.97 ± 0.33	11.85 ± 0.42	0.742 ± 0.042	2.8 ± 5.8
	2	77	−15.816 ± 0.008	−12.063 ± 0.008	0.7627 ± 0.0009	0.08 ± 0.3
	3	2	15.752 ± 0.112	12.044 ± 0.084	0.765 ± 0.011	−0.17 ± 1.9
CeO_2	4	300	15.21 ± 0.28	11.62 ± 0.28	0.764 ± 0.032	−0.09 ± 4.7
	5	14	15.809 ± 0.005	12.048 ± 0.003	0.7621 ± 0.0004	0.16 ± 0.51
BaO	6	77	14.38 ± 0.56	10.96 ± 0.56	0.762 ± 0.069	0.14 ± 9
MgO	7	Room	15.17 ± 0.15	11.542 ± 0.15	0.761 ± 0.017	0.32 ± 2.7
CaO	8	•••	16.1 ± 0.3	12.35 ± 0.3	0.767 ± 0.006	−0.5 ± 4.8
$CaWO_4$	9	77	16.2 ± 0.055	12.40 ± 0.055	0.7654 ± 0.006	−0.28 ± 1.2
$ZrSiO_4$	10	300	16.922 ± 0.084	12.907 ± 0.055	0.7627 ± 0.007	0.07 ± 1.3
	11	290	12.63 ± 0.027	9.67 ± 0.027	0.7656 ± 0.004	−0.3 ± 0.95
$HfSiO_4$	10	300	17.006 ± 0.055	12.964 ± 0.055	0.7623 ± 0.0057	0.13 ± 1.2
$ThSiO_4$	10	300	16.643 ± 0.055	12.657 ± 0.055	0.7605 ± 0.0058	0.37 ± 1.2
$CaCO_3$	12	77	15.897 ± 0.012	12.122 ± 0.013	0.7625 ± 0.0014	0.1 ± 0.64
BMDN	13	2	16.486 ± 0.003	12.559 ± 0.002	0.76180 ± 0.00026	0.2 ± 0.5
	14	77	14.89 ± 0.48	11.15 ± 0.84	0.749 ± 0.08	1.9 ± 11
LES	15	77	18.26 ± 0.37	14.59 ± 0.37	0.799 ± 0.037	−4.7 ± 5.3
	15	4	18.10 ± 0.22	14.33 ± 0.22	0.791 ± 0.022	−3.7 ± 3.4
YPO_4	16	Room	−16.98 ± 0.08	−13.02 ± 0.08	0.7668 ± 0.0083	−0.45 ± 0.63
GdN(nmr)	17	4	19.567	14.734	0.753 ± 0.004	1.35 ± 1.03
atom Gd(opt)	18	•••	•••	•••	0.80 ± 0.02	−4.8 ± 3.1
atom Gd(opt)	19	•••	•••	•••	0.79 ± 0.02	−3.5 ± 3.1
atom Gd(beam)	20	•••	•••	•••	0.76252 ± 0.00013	0.102 ± 0.48

[a]Some data for this table are taken from Refs. 59 and 15. If no technique is mentioned EPR or ENDOR was used.

[b](1) Ref. 80; (2) Ref. 48; (3) Ref. 31; (4) I. V. Vinokurov, Z. N. Zonn, and V. A. Ioffe, Sov. Phys.-Solid State 7, 814 (1965); (5) Ref. 59; (6) K. E. Mann and I. V. Holroyd, Phys. Status Solidi 28, K27 (1968); (7) M. M. Abraham, L. A. Boatner, Y. Chen, J. L. Kolopus, and R. W. Reynolds, Phys. Rev. B 4, 2853 (1971); (8) A. T. Omlinson, thesis University of Keele 1968; (unpublished); (9) C. F. Hempstead and K. D. Bowers, Phys. Rev. 118, 131 (1960); (10) M. M. Abraham, G. W. Clark, C. B. Finch, R. W. Reynolds, and H. Zeldes, J. Chem. Phys. 50, 2057 (1969); (11) D. R. Hutton and G. J. Troup, Brit. J. Appl. Phys. 15, 405 (1964); (12) S. A. Marshall and R. A. Serway, Phys. Rev. 171, 345 (1968); (13) Ref. 54; (14) W. Low, Phys. Rev. 103, 1309 (1956); (15) This work; (16) Ref. 67; (17) E. L. Boyd and R. J. Gambino, Phys. Rev. Lett. 12, 20 (1964); (18) Ref. 70; (19) Ref. 69; (20) Ref. 72.

[c]Δ was calculated using a ratio of g_n factors of 0.7633 ± 0.0035 from Ref. 59.

limits on Δ are not as yet small enough for a meaningful decision about the extent of core polarization in Gd^{3+} to be made. Such a determination must await more precise experiments to measure the various contributions to A, and must await accurate unrestricted Hartree-Fock and relativistic wave functions to calculate these contributions from first principles.

It is unfortunate that the ZFPMR experimental error is greater than the difference between the measured A values for 77 and 4 K. Theories have been developed for the temperature dependence of the hyperfine constant for S-state ions,[61] which yield a 2% decrease in A for Eu^{2+} in CaF_2 on going from 4 to 77 K, due to temperature-dependent configuration mixing by the orbit-lattice interaction. ZFENDOR should allow precise enough measurements to determine temperature dependence for lower than cubic symmetry by reducing the problem of broad lines in LES. Of course, this temperature dependence may be especially well studied in ThO_2 and BMDN for which magnetic resonance lines are considerably sharper than in LES.

2. *Quadrupole interaction*

The electric-quadrupole term in the Hamiltonian represents the energy of interaction of the electric-field gradient (EFG) at the nucleus with the nuclear-electric-quadrupole moment and is written as[62]

$$eq = eq_c(1-\gamma_\infty) + eq_v(1-R_q)\ , \qquad (4.3)$$

in which eq_c is the EFG due to the external crystal field about the ion, eq_v is the EFG due to the valence-shell electrons, and e is the charge on the electron. The two parameters γ_∞ and R_q are Sternheimer antishielding factors which account for the effect of distortion of the closed shells of electrons by the gradients. They may have either sign and hence may reverse the direction of the field gradient.

Since q_c is proportional to the quadrupolar crystal-field parameter A_2^0, it must vanish in cubic

symmetry. (A discussion of the relation between A_l^m's and B_l^m's can be found in Ref. 40.) Many of the hosts in Table X are cubic, and hence observation of a small quadrupole term in their EPR would be due to the second part of Eq. (4.3). However, in the nonrelativistic limit of LS coupling, the second term in Eq. (4.3) would also vanish[63] due to the spherical symmetry of the half-filled shell. We know of only one case for which a quadrupolar-interaction term has been measured for Gd^{3+} in cubic symmetry; namely, the ENDOR investigation in ThO_2 by Hurrell.[64] He was able to obtain spectra for the $^{157}Gd^{3+}$ isotope only and measured the quadrupole constant for the appropriate cubic spin Hamiltonian[60] $B = -0.687 \pm 0.18$ MHz. The other two rare-earth S-state ions have somewhat larger constants.[62,65]

Evans, Sandars, and Woodgate[66] have calculated the various contributions to the quadrupolar constant for the S-state atoms, ^{55}Mn, and both odd europium isotopes. They ascribe nonzero contributions to the quadrupole interaction to a breakdown of LS coupling, and to a breakdown of the nonrelativistic approximation. Using relativistic wave functions it is possible to calculate a contribution called the Casimir effect indicated by $B_{\mathrm{Cas.}}$, which in both cases was found to dominate the breakdown of LS coupling.

Since the quadrupole interaction is so small in cubic symmetry for which the first part in Eq. (4.3) vanishes, it may be expected that the first term will dominate the second in symmetry lower than cubic. There are only three cases for which this interaction has been measured. Using a standard quadrupole term of the form $P[I_z^2 - \frac{1}{3}I(I+1)]$, Danner, Ranon, and Stamires[9] and Rannon and Stamires[67] were able to measure $|^{157}P| = 53.7 \pm 0.3$ MHz and $|^{155}P| = 50.4 \pm 0.3$ MHz in YPO_4 by ordinary EPR. It is interesting to note that the ZFPMR studies of Kahle *et al.*[68] did not reveal the existence of hyperfine structure in the spectrum of this salt. Using high-field ENDOR, Butti *et al.*[54] measured $^{157}P = 26.527 \pm 0.003$ MHz and $^{155}P = 24.905 \pm 0.002$ MHz in BMDN. For convenience, the value obtained in this work is restated: $^{157}P = -53.09 \pm 0.76$ MHz and $^{155}P = -51.16 \pm 0.76$ MHz in LES. The relatively large reported error (3σ) is mostly determined by the linewidth of Gd^{3+} transitions in LES.

P may be written as $3Qe^2q/4I(2I-1)$. Hence, a ratio of P values for two isotopes should equal the ratio of quadrupole moments for each, if they have the same spin and are positioned in the same EFG. Thus one can compare the ratio of P's with the ratio of nuclear-electric-quadrupole moments, $R(Q) \equiv {}^{157}Q/{}^{155}Q$. There are four measurements of $R(Q)$. They are the optical determination by Kaliteevski[69] of 1.28 ± 0.02, the optical determination by Speck[70] of 0.80 ± 0.02, the Mössbauer determination by Prange[71] of 0.78 ± 0.06, and the accurate atomic beam measurement by Unsworth[72] of 1.06534 ± 0.00003.

The ratio of P values, $R(P) \equiv {}^{157}P/{}^{155}P$, from above are 1.065 ± 0.012 for YPO_4, 1.06513 ± 0.00021 for BMDN, and 1.038 ± 0.030 for LES. The optical determinations are mutually inconsistent. Even though one of them is consistent with the Mössbauer value, all three are inconsistent with the accurate beam value. Moreover, all three $R(P)$'s agree with the beam measurement within experimental error.

It is interesting to note that except possibly for sign, the P values for YPO_4 and LES agree with each other within experimental error. If eq_c were the only gradient contributing to the quadrupole term, then the A_2^0 values for each salt would have to be the same if γ_∞ were the same for both. In fact, estimates lead one to conclude that this is roughly correct with $90\ \mathrm{cm}^{-1} \leq A_2^0\langle r^2\rangle \leq 100\ \mathrm{cm}^{-1}$ for both YPO_4 and LES.[73] While b_2^0 for these systems are quite different [$b_2^0(YPO_4) \approx 3.5\, b_2^0(\mathrm{LES})$] it must be remembered that A_2^0 is the important crystal-field parameter for the quadrupole-interaction constant. It can be demonstrated that the relationship between these two parameters is neither direct nor simple. Indeed, higher-order and indirect terms may invalidate lattice summations and even simple decomposition of mechanisms; it is perhaps possible that in low-symmetry (noncubic) crystals an apparent q_v is enhanced. This latter point would most simply explain the fact that $|P(YPO_4)| = |P(\mathrm{LES})|$ for Gd^{3+}. It would be particularly useful if ZFPMR could be employed to obtain a sign for P in YPO_4.

Finally, it is appropriate to inquire whether the quadrupole coefficients for LES are of about the right magnitude in an absolute sense. The EFG at the La^{3+} nucleus of diamagnetic LES has been measured by NMR and, based on this determination, a procedure has been developed for estimating the ionic contribution to P for any lanthanide ion in LES.[74] Also, the lattice contribution to P, $P_{\mathrm{latt.}}$, for $^{159}Gd^{3+}$ in neodynium ethylsulfate (NdES) has been measured by nuclear-alignment techniques.[75] Block and Shirley[75] find $P_{\mathrm{latt.}}$ for $^{159}Gd^{3+}$ to be -43.2 ± 1.5 MHz for ^{159}Gd in NdES using a quadrupole moment of 1.56 b. Since this isotope has the same spin as those of interest here, one may predict ^{155}P equal to -44.0 ± 7.3 MHz using $^{155}Q = 1.59 \pm 0.16$ b.[72] Considering the approximations in the above calculation and the fact that the host lanthanide ion is different, observed and predicted magnitude and absolute sign of P are judged to be in agreement.

It is possible to evaluate P in another way. If A_2^0 is a quadrupolar-lattice sum, one can write (using the notation of Edmonds[74])

$$P_{\text{latt.}} = 3QA_2^0\gamma_N/I(2I-1)\,, \qquad (4.4)$$

in which $\gamma_N = 1 - \gamma_\infty$ and is assumed to be ± 21.5 for LES. The negative sign is usually chosen to agree with antishielding calculations. Experimental crystal-field parameters from optical experiments are defined as $V_2^0 = \gamma_E A_2^0 \langle r^2 \rangle$. $\langle r^2 \rangle$ is the expectation value of the radius of the open-shell $4f$ electrons. Edmonds's $\gamma_E A_2^0$ is equal to Freeman and Watson's[76] A_2^0. Powell and Orbach[77] obtain $V_2^0 = 100.6$ cm^{-1} and Freeman and Watson's best Hartree-Fock estimate of $\langle r^2 \rangle$ is $0.785 a_0^2$; $\gamma_E A_2^0$ for Gd then becomes $128 a_0^{-2}$ cm^{-1} (a_0 is the Bohr radius). Finally, Edmonds estimates $\gamma_N(\text{La})/\gamma_E(\text{La})$ equal to -550, which yields $A_2^0\gamma_N(\text{Gd}) = -550 A_2^0\gamma_E(\text{Gd}) = (-7.04\times 10^4) a_0^{-2}$ cm^{-1}. Therefore, with the measurement of $^{155}Q = 1.59 \pm 0.16$ b, a value of $^{155}P_{\text{latt.}}$ equal to -110 MHz obtains.

This estimate is just over a factor of 2 from our measurements of ^{155}P. Allowing for generous error limits at each step in the above procedure, and allowing for the fact that no account of q_v has been made, once again the measured value and sign of P appear reasonable. For gadolinium in crystals of less than cubic symmetry, the hyperfine spectrum may be expected to be dominated by the quadrupole interaction, in contrast to the more usual situation, for which P is much smaller than A. This quadrupole interaction is composed almost exclusively from lattice contributions.

V. LINEWIDTHS

Linewidths for Gd-doped LES are essentially the same for ZFPMR transitions as EPR transitions (~ 20–30 MHz). Thus, inhomogeneity in the external field contributes in only a small way to the linewidth. Also, since the linewidth is largely independent of temperature and the strength of the external field, one may rule out broadening by spin-lattice relaxation as the cause of broad lines. Indeed, the observed linewidth of 25 MHz sets a 12.7 nsec lower bound on the relaxation times. The spin-lattice relaxation time has been investigated by several workers[78] and found to be four or five orders of magnitude slower than this lower limit. The linewidth of gadolinium in various hosts is known to depend on concentration, at concentrations above about 0.1 mole%.[79,80]

The residual linewidth in LES is caused by inhomogeneous broadening of the resonance line; this broadening is much greater than in other hosts. One can presume it to result from two factors; namely, the statistical variation of the crystal-field parameters due to lattice strains and dipolar interaction with the neighboring nuclear moments.

On this basis, then, one might be willing to suggest that the broadening in gadolinium-doped LES must be entirely due to dipolar broadening. This is, however, not the case, as Nd-doped LES shows a linewidth of 8–10 MHz for many of its lines.[4,10] Since transitions are not observed between crystal-field levels in Nd (the first low-lying crystal-field level is 100 cm^{-1} above the ground state), inhomogeneties in the crystal potential must play a greatly reduced role in the Nd line broadening. Hence a major part of the linewidth for gadolinium must arise from variation in the crystal field. If relaxation times contributed significantly to the linewidth, one would expect Nd to have wider lines than Gd because the relaxation time of the former is considerably faster.

The effect of the surrounding nuclear magnetic moments associated with water of hydration in LES can be seen in several ways. The linewidth of Gd-doped BMDN is on the order of 10 MHz. This comparative sharpness can be explained by the fact that there are only six neighboring nitrogens in BMDN, but there are 18 neighboring protons in LES. Additionally, the magnetic moment of ^{14}N is seven times smaller than that of ^{1}H. The protons of the water molecules are tightly coupled to the gadolinium ion, since one may observe their dynamic nuclear orientation.[36] Sharpening of the spectrum on deuteration is accounted for by the magnetic moment of the deuteron being 3.25 times smaller than that of the proton. The fact that there is only a 20–50% sharpening is probably associated with the substantial inhomogeneties of the crystal field in LES. It is thus clear that both dipolar and crystal-field mechanism contribute roughly equally to the observed Gd^{3+} in LES zero-field linewidth.

In the series of ethylsulfates in which the host ion is varied, a great variety of linewidths are observed. In this instance observed linewidths are a complicated function of the magnetic moment and relaxation time of the host lanthanide. The detailed explanation of the trends as a function of host, temperature, and transition involved must await a suitable theory for paramagnetic relaxation of rare-earth S-state ions in either zero or high field.

VI. CONCLUSION

Both crystal-field and hyperfine interactions in Gd^{3+}-doped LES hydrate have been studied. It was shown that the zero-field spin Hamiltonian agrees with the high-field spin Hamiltonian to a higher degree of accuracy than has previously been achieved. The available signal-to-noise ratio enabled both the magnitude and absolute sign of the dipole- and electric-quadrupole hyperfine interaction constants for this system to be determined for the first time. These constants had previously gone unobserved during 23 years of conventional EPR experiments. These parameters were discussed from the viewpoint of the theory of hfs, and

their magnitudes and signs were argued to be reasonable in comparison with other systems. Indeed, it is shown that for systems of lower than cubic symmetry, the quadrupole interaction should dominate the dipole interaction in the spectrum. While the size of P can be determined in high field by placing $\vec{H}$ perpendicular to the crystal symmetry axis, its sign remains indeterminate except at extremely low temperatures (~ 0.001 K).

Finally, a previously unnoticed effect was reported. The crystal field parameters of gadolinium in various lanthanide ethylsulfates change on deutera tion of the waters of hydration. Some mechanisms were discussed which cause this change as well as linewidths for the isomorphic series of lanthanide ethylsulfates. For the diamagnetic LES the Gd^{3+} linewidths are shown to arise from at least two separate and distinct factors; crystal-field inhomogeneities and magnetic dipole-dipole (local-field) coupling with neighboring nuclei.

---

*Supported in part by grants from The Research Corporation, Army Research Office-Durham, Office of Naval Research, and the National Science Foundation.

†Presented in part at the *Twenty-ninth Symposium on Molecular Structure and Spectroscopy*, 10 June 1974 (Paper TD9).

‡Present address: Department of Chemistry, Massachusetts Institute of Technology, Cambridge, Massachusetts 02139.

[1]E. R. Bernstein and G. M. Dobbs, Rev. Sci. Instrum. 44, 1314 (1973).

[2]S. A. Marshall, S. V. Nistor, C. Y. Huang, and T. Marshall, Phys. Status Solidi B 59, 55 (1973).

[3]E. R. Bernstein and D. S. Franceschetti, Phys. Rev. B 9, 3678 (1974).

[4]L. E. Erickson, Phys. Rev. 143, 295 (1966).

[5]J. M. Baker, W. Hayes, and M. C. M. O'Brien, Proc. R. Soc. Lond. A 254, 273 (1960).

[6]R. W. Brandon, R. E. Gerkin, and C. A. Hutchison, J. Chem. Phys. 37, 447 (1962).

[7]C. A. Hutchison, Jr., in *The Triple State*, edited by A. B. Zahlan (Cambridge U. P., Cambridge, England, 1967), p. 63; C. A. Hutchison, Jr., S. V. Nicholas, and G. W. Scott, J. Chem. Phys. 53, 1906 (1970).

[8]M. A. El-Sayed, in *MTP International Review of Science-Physical Chemistry*, edited by A. D. Buckingham and D. A. Ramsay (Butterworths, London, 1972), Ser. 1, Vol. 3, p. 119.

[9]J. C. Danner, U. Ranon, and D. N. Stamires, Phys. Rev. B 3, 2141 (1971).

[10]E. R. Bernstein and G. M. Dobbs (unpublished); G. M. Dobbs, Ph. D. thesis (Princeton University, 1974), (unpublished).

[11]G. F. Koster and H. Statz, Phys. Rev. 113, 445 (1959); H. Statz and G. F. Koster *ibid.* 115, 1568 (1959); F. K. Kneubühl, Phys. Kondens. Mater. 1, 410 (1963); T. Ray, Proc. R. Soc. Lond. A 277, 76 (1964); H. Wu-Han, L. Fu-Cheng and Z. Ji-Kang, Proc. Phys. Soc. Lond. 84, 661 (1964); W. J. C. Grant and M. W. P. Strandberg, J. Phys. Chem. Solids 25, 635 (1964); F. K. Kneubühl, Phys. Kondens. Mater. 4, 50 (1965); A. Bieri and F. K. Kneubühl, *ibid.* 4, 230 (1965); G. A. Woonton and G. L. Dyer, Can. J. Phys. 45, 2265 (1967); J. S. M. Harvey and H. Kiefte, J. Phys. B 3, 1326 (1970).

[12]S. Geschwind, in *Hyperfine Interactions*, edited by A. J. Freeman and R. B. Frankel (Academic, New York, 1967), p. 225.

[13]A. Abragam and B. Bleaney, *Electron Paramagnetic Resonance of Transition Ions* (Clarendon, Oxford, England, 1970).

[14]See, for example, G. H. Dieke, *Spectra and Energy Levels of Rare Earth Ions in Crystals* (Interscience, New York, 1968).

[15]H. A. Buckmaster and Y. H. Shing, Phys. Status Solidi A 12, 325 (1972).

[16]M. M. Abraham, L. A. Boatner, C. B. Finch, E. J. Lee, and R. A. Weeks, J. Phys. Chem. Solids 28, 81 (1967).

[17]H. A. Buckmaster, R. Chatterjee, and Y. H. Shing, Can. J. Phys. 50, 991 (1972).

[18]Through this paper all ± numbers are rms errors, defined as three times the standard devation σ.

[19]B. G. Wybourne, Phys. Rev. 148, 317 (1966).

[20]T. J. Menne, J. Phys. Chem. Solids 28, 1629 (1967); C. Y. Huang, Phys. Rev. 159, 683 (1967); T. J. Menne *ibid.* 170, 356 (1968); P. Schlottman and M. C. G. Passeggi, Phys. Status Solidi B 52, K107 (1972); H. Bill, R. Chatterjee, and J. M. Dixon, *ibid.* B 57, K51 (1973); T. Lulek, Acta Phys. Pol. 36, 551 (1969); T. Lulek, Phys. Status Solidi 39, K105 (1970); H. A. Buckmaster, R. Chatterjee, and Y. H. Shing, Can. J. Phys. 50, 78 (1972); D. J. Newman and M. M. Ellis, Phys. Lett. 23, 46 (1966); D. J. Newman, Chem. Phys. Lett. 6, 288 (1970); D. R. Johnston, E. Y. Wong, and O. M. Stafsudd, J. Chem. Phys. 44, 2693 (1966).

[21]D. J. Newman and W. Urban, J. Phys. C 5, 3101 (1972).

[22]D. J. Newman, J. Phys. C 6, L271 (1973); Adv. Phys. 20, 197 (1971).

[23](a) J. A. A. Ketelaar, Physica 4, 619 (1937); (b) D. R. Fitzwater and R. E. Rundle, Z. Kristallogr. 112, 362 (1959).

[24]R. J. Elliott and K. W. H. Stevens, Proc. Phys. Soc. Lond. A 64, 205 (1951).

[25]B. Bleaney, R. J. Elliott, and H. E. D. Scovil, Proc. Phys. Soc. Lond. A 64, 933 (1951).

[26]B. Bleaney, R. J. Elliott, H. E. D. Scovil, and E. S. Trenam, Philos. Mag. 42, 1062 (1951).

[27]R. J. Elliott and K. W. H. Stevens, Proc. R. Soc. Lond. A 219, 387 (1953).

[28]B. Bleaney, H. E. D. Scovil, and R. S. Trenam, Proc. R. Soc. Lond. A 223, 15 (1954).

[29]H. A. Buckmaster, Can. J. Phys. 34, 150 (1956); 34, 341 (1956).

[30]H. A. Buckmaster, in *Paramagnetic Resonance, Proceedings of the First International Conference, Jerusalem*, 1962, edited by W. Low (Academic, New York, 1963), Vol. 1, p. 217.

[31]M. M. Abraham, E. J. Lee, and R. A. Weeks, J. Phys. Chem. Solids 26, 1249 (1965).

[32]J. Dweck and G. Seidel, Phys. Rev. 151, 289 (1966).

[33]H. A. Buckmaster and Y. H. Shing, *Proceedings of the Seventh Rare Earth Research Conference*, 1968 (Natl. Tech. Info. Ser., Washington, D.C., 1969), Vol. 1, p. 323.
[34]C. R. Viswanthan and E. Y. Wong, J. Chem. Phys. 49, 966 (1968).
[35]I. R. Dagg, R. C. Kemp, and H. F. Symmons, J. Phys. C 2, 1098 (1969).
[36]R. J. Richardson, Ph.D. thesis (St. Louis University, 1969) (unpublished); R. J. Richardson and S. Lee, Phys. Rev. B 1, 108 (1970).
[37]R. E. Gerkin and D. L. Thorsell, J. Chem. Phys. 57, 2665 (1972).
[38]R. E. Gerkin and D. L. Thorsell, J. Chem. Phys. 57, 188 (1972).
[39](a) H. A. Buckmaster, R. Chatterjee, and Y. H. Shing, J. Phys. C 4, 832 (1971); (b) H. A. Buckmaster, R. Chatterjee, and Y. H. Shing, J. Mag. Res. 4, 85 (1971).
[40]M. T. Hutchings, in *Solid State Physics*, edited by F. Seitz and D. Turnbull (Academic, New York, 1964), Vol. 16, p. 227.
[41]D. H. Templeton and C. H. Dauben, J. Am. Chem. Soc. 76, 5237 (1954).
[42]W. C. Hamilton and J. A. Ibers, *Hydrogen Bonding in Solids* (Benjamin, New York, 1968).
[43]W. C. Hamilton and J. A. Ibers, Acta Crystallogr. 16, 1209 (1963).
[44]R. G. Delaplane, J. A. Ibers, J. R. Ferraro, and J. J. Rush, J. Chem. Phys. 50, 1920 (1969).
[45]W. Hillmer and W. Urban, Phys. Status Solidi 39, 527 (1970).
[46]P. Nowicki, W. Hillmer, and W. Urban, Phys. Status Solidi B 47, 549 (1971).
[47]G. Burns, Phys. Rev. 128, 2121 (1962); J. Chem. Phys. 42, 377 (1965).
[48]S. A. Marshall, Phys. Rev. 159, 191 (1967).
[49]P. Diehl, H. Kellerhals, and E. Lusting, in *NMR Basic Principles and Progress*, edited by P. Diehl, E. Fluck, and R. Kosfeld (Springer Verlag, New York, 1972), Vol. 6, p. 1.
[50]H. A. Buckmaster, J. C. Dering, and D. J. I. Fry, J. Phys. C 1, 599 (1968).
[51]J. E. Lowther, Phys. Status Solidi B 46, K19 (1971).
[52]M. L. Meil'man, Fiz. Tverd. Tela 14, 3055 (1972) [Sov. Phys.-Solid State 14, 2612 (1972)].
[53]A. Zalkin, J. D. Forrester, and D. H. Templeton, J. Chem. Phys. 39, 2881 (1963). The reason for the sharp lines compared to the ethylsulfates is not understood, except to say that since the trivalent gadolinium is surrounded by the nitrate groups, its nearest neighbors are not hydrogen bonded. The Gd^{3+} substitutes for the trivalent bismuth and the structure may be considered as $[Bi(NO_3)_6]_2\,[Mg(H_2O)_6]_3 \cdot 6H_2O$.
[54]C. H. Butti, C. A. Swarts, D. van Ormondt, and R. deBeer, Phys. Lett. A 45, 247 (1973).
[55]S. Misumi, T. Isobe, and T. Higa, Nippon Kagaku Kaishi 1973, 2039 (1973).
[56](a) R. E. Trees, Phys. Rev. 92, 308 (1953); (b) A. Abragam, J. Horowitz, and M. H. L. Pryce, Proc. R. Soc. Lond. A 230, 169 (1955); (c) C. Schwartz, Phys. Rev. 97, 380 (1955); Phys. Rev. 105, 173 (1957); (d) S. M. Blinder, Adv. Quantum Chem. 2, 47 (1965); (e) P. G. H. Sandars and J. Beck, Proc. R. Soc. Lond. A 289, 97 (1966).
[57]C. M. Moser, in *Hyperfine Interactions*, edited by A. J. Freeman and R. B. Frankel (Academic, New York, 1967), p. 95.
[58]B. Bleaney, Colloq. Int. Cent. Natl. Rech. Sci. 164, 13 (1966).
[59]J. M. Baker, G. M. Copland, and B. M. Wanklyn, J. Phys. C 2, 862 (1969).
[60]J. M. Baker and F. I. B. Williams, Proc. R. Soc. Lond. 267, 283 (1962).
[61]T. J. Menne, Phys. Rev. 180, 350 (1969); T. J. Menne, D. P. Ames, and S. Lee, *ibid.* 169, 333 (1968).
[62]R. E. Watson and A. J. Freeman, in *Hyperfine Interactions*, edited by A. J. Freeman and R. B. Frankel (Academic, New York, 1967), p. 53.
[63]B. Bleaney, in *Hyperfine Interactions*, edited by A. J. Freeman and R. B. Frankel (Academic, New York, 1967), p. 1.
[64]J. P. Hurrell, Brit. J. Appl. Phys. 16, 755 (1965).
[65]J. M. Baker, J. R. Chadwick, G. Garton, and J. P. Hurrell, Proc. R. Soc. Lond. A 286, 352 (1965).
[66]L. Evans, P. G. H. Sandars, and G. K. Woodgate, Proc. R. Soc. Lond. A 289, 108, 114 (1966).
[67]U. Ranon and D. N. Stamires, Chem. Phys. Lett. 5, 221 (1970).
[68]H. G. Kahle, V. Koch, J. Plamper, and W. Urban, J. Chem. Phys. 49, 2702 (1968); H. G. Kahle, H. C. Schopper, W. Urban, and W. Wüchner, Phys. Status Solidi 38, 815 (1970).
[69]N. I. Kaliteevski, M. P. Chaika, I. Kh. Pacheva, and E. E. Fradkin, Zh. Eksp. Teor. Fiz. 37, 882 (1959) [Sov. Phys.—JETP 10, 629 (1960)].
[70]D. R. Speck, Phys. Rev. 101, 1725 (1956).
[71]H. Prange, Z. Phys. 212, 415 (1968).
[72]P. J. Unsworth, J. Phys. B 2, 122 (1969).
[73]Compare Ref. 13, p. 304 and 305 with D. Kruse, Z. Phys. 203, 49 (1967); W. Hintzmann, *ibid.* 230, 213 (1970); C. Brecker, H. Samelson, R. Riley, and A. Lewpicki, J. Chem. Phys. 49, 303 (1968).
[74]D. T. Edmonds, Phys. Rev. Lett. 10, 129 (1963).
[75]J. Block and D. A. Shirley, J. Chem. Phys. 39, 1128 (1963); Phys. Rev. 143, 278 (1966).
[76]A. J. Freeman and R. E. Watson, Phys. Rev. 127, 2058 (1962).
[77]M. J. D. Powell and R. Orbach, Proc. Phys. Soc. Lond. 78, 753 (1961).
[78]G. Feher and H. E. D. Scovil, Phys. Rev. 105, 760 (1957); C. F. Davis, Jr., M. W. P. Strandberg, and R. L. Kyhl, *ibid.* 111, 1268 (1958); G. V. Marr and P. Swarup, Can. J. Phys. 38, 495 (1960); S. A. Peskovatskii and A. N. Chernets, Fiz. Tverd. Tela 4, 657 (1962); 4, 665 (1972). [Sov. Phys.-Solid State 4, 479 (1962); 4, 484 (1962)].
[79]Yu E. Pol'skii, Fiz. Tverd. Tela 6, 842 (1964) [Sov. Phys.-Solid State 6, 651 (1964)].
[80]W. Low and D. Shaltiel, J. Phys. Chem. Solids 6, 315 (1958). It is a general feature of S-state ion high-field spectra that linewidths increase for higher M_S values, due to the increasing effect of the crystal field.